Experimental Evaluation of Bayesian Image Reconstruction Combined with Spatial-Superresolution and Spectral Reflectance Recovery

Yusuke Murayama, Pengchang Zhang and Ari Ide-Ektessabi
Graduate School of Engineering, Kyoto University, Kyoto, Japan

Keywords: Multispectral Image, Spectral Reflectance Recovery, Image Superresolution, Bayesian Estimation, Digital Archiving.

Abstract: Acquisition of a multispectral image and analysis of the object based on spectral information recovered from the image has recently received attention in digital archiving of cultural assets. However multispectral imaging faces such problems as long image acquisition time and severe registration between band images. In order to solve them, we have proposed an extended method combining Bayesian image superresolution with spectral reflectance recovery. In this study we evaluated quantitatively the performance of the proposed technique using a typical 6-band multispectral scanner and a Japanese painting. The accuracy of recovered spectral reflectance was investigated with respect to the ratio of the capturing resolution to the recovering resolution. The experimental result indicated that the spatial resolution can be increased by around 1.7 times, which means image capturing time can be reduced almost by one third and besides the angle of view can be extended by 1.7 times.

1 INTRODUCTION

A multispectral imaging device such as a multispectral camera or scanner is a preferable tool for digital archiving of cultural assets: paintings, documents, textile fabrics and other art works. The first reason is that a multispectral image has the ability to produce color with higher-fidelity than a commonly-used trichromatic image (Yamaguchi et al., 2002). Second, the higher spectral resolution of a multispectral image enables recovering spectral reflectance in visible region of the object and then analyzing spectroscopic properties (DiCarlo and Wandell, 2003; Shimano et al., 2007). One example is pigment identification based on the recovered spectral reflectance of paintings (Pelagotti and Mastio, 2008; Toque et al., 2009), and such applications have recently received increasing attention.

A typical multispectral camera is made up of a monochromatic camera, light source for illuminant and band-pass filters which transmit radiation of selected wavelengths (Fukuda et al., 2005; Shimano et al., 2007). Similarly, a typical multispectral scanner can be assembled from monochromatic scanner (Toque et al., 2009). Band images represented as monochromatic images are captured sequentially by attaching different band-pass filters to the front of the camera, thus forming a multispectral image.While the band number of a trichromatic camera or scanner is fixed to three of red, green, and blue, that of a multispectral camera or scanner can be easily increased as necessary.

Unfortunately, long acquisition time and image registration make multispectral image acquisition a demanding work. A half dozen to a dozen of color filters are required to recovery spectral reflectance so it takes a time several or more times longer to obtain a multispectral image than capturing a trichromatic image. The situation becomes even worse when dealing with large-size objects or high spatial resolutions. Another problem is subpixel level position shifts between band images caused by the small translation of camera in changing a filter or the mechanical error of starting position of scanner. Such misregistration declines color accuracy especially along edge lines, and leads to incorrect recovery of spectral reflectance.

In order to overcome them, we have proposed an extended method for recovering spectral reflectance and increasing spatial resolution simultaneously, namely Bayesian image reconstruction combined with spatial-superresolution and spectral reflectance recovery (Murayama and Ide-Ektessabi, 2012). Image superresolution refers to an image processing technique which increases the spatial resolu-

Murayama Y., Zhang P. and Ide-Ektessabi A..
Experimental Evaluation of Bayesian Image Reconstruction Combined with Spatial-Superresolution and Spectral Reflectance Recovery.
DOI: 10.5220/0004346001390142
In *Proceedings of the International Conference on Computer Vision Theory and Applications* (VISAPP-2013), pages 139-142
ISBN: 978-989-8565-47-1

tion for a set of images sampling the same object with different spatial points in sub-pixel levels. The application of image superresolution avoids the misregistration band captured images and besides makes itself a chance for increasing spatial resolution. The significant decrease in acquisition time of a multispectral image derives from the fact that image superresolution allows capturing band images at lower spatial resolution than the required resolution. If the spatial resolution of image capturing is reduced by half, the camera's exposure time or scanning time can be reduced by quarter, and the angle of view becomes twice as wide.

The purpose of this study is to evaluate the quantitative accuracy of the proposed method and indicate its effectiveness. An experiment was conducted using a typical 6-bands multispectral scanner and a Japanese painting. Sets of band images were captured with different spatial resolutions, and then errors of recovered spectral reflectance with a certain resolution were evaluated.

2 PROPOSED BAYESIAN IMAGE RECONSTRUCTION

In this section, We outline Bayesian image reconstruction combined with spatial-superresolution and spectral reflectance recovery (Murayama and Ide-Ektessabi, 2012).

Let $\{\mathbf{y}_k\}_{k=1}^K$ be a multispectral image which consists of K band images with $W_L \times H_L = N_L$ pixels, and $\{\mathbf{x}_t\}_{t=1}^T$ be a hyperspectral image of the same object with T spectral samplings and $W_H \times H_H = N_H$ pixels. Here, $\mathbf{y}_k$ is a monochromatic image acquired by using the k-th band-pass filter and, $\mathbf{x}_t$ is also a monochromatic image which represents reflectance at wavelength λ_t. These monochromatic images are vectorized in lexicographical order. We denotes the fully vectorized images of $\{\mathbf{y}_k\}_{k=1}^K$ and $\{\mathbf{x}_t\}_{t=1}^T$ by

$$\mathbf{y} = \begin{bmatrix} \mathbf{y}_1 \\ \vdots \\ \mathbf{y}_K \end{bmatrix}, \quad \mathbf{x} = \begin{bmatrix} \mathbf{x}_1 \\ \vdots \\ \mathbf{x}_T \end{bmatrix}. \tag{1}$$

This method recovers $\{\mathbf{x}_t\}_{t=1}^T$ from $\{\mathbf{y}_k\}_{k=1}^K$ under the following conditions: a) $T > K$. b) $\frac{W_H}{W_L} = \frac{H_H}{H_L} = r > 1$, where r is the rate of superresolution. c) each band image $\mathbf{y}_k$ of the multispectral image includes a small amount of position shift to other band images, but the hyperspectral image $\{\mathbf{x}_t\}_{t=1}^T$ is completely registered.

The likelihood of $\{\mathbf{x}_t\}_{t=1}^T$ is derived from a linear model of multispectral image acquisition by

$$\begin{aligned} p(\{\mathbf{y}_k\}_{k=1}^K|\{\mathbf{x}_t\}_{t=1}^T) &= \prod_{k=1}^K p(\mathbf{y}_k|\{\mathbf{x}_t\}_{t=1}^T) \\ &= \prod_{k=1}^K \mathcal{N}\left(\mathbf{y}_k|(\mathbf{a}_k^T \otimes B_k)\mathbf{x}, \beta I_{N_L}\right), \end{aligned} \tag{2}$$

where a T-dimensional vector $\mathbf{a}_k$ represents the system sensitivity of the k-th band, a N_L-by-N_H matrix B_k spatial degradations: geometrical transform, blurring, and downsampling, β the variance of the sensor noise, $\otimes$ the Kronecker product, and $\mathcal{N}(\mathbf{z}|\mu,\Sigma)$ the multivariate Gaussian distribution of $\mathbf{z}$ whose mean and covariance matrix are μ and *varSigma*. $\mathbf{a}_k$ is the product of the following functions at the same sampling points as $\{\mathbf{x}_t\}_{t=1}^T$: spectral sensitivity of the camera and spectral transmittance of the attached filter and spectral power distribution of the light source. B_k depends on the point correspondences between $\mathbf{y}_k$ and $\{\mathbf{x}_t\}_{t=1}^T$, and the point spread function of blurring (PSF). In this study, we assumed position shifts in rotation and translation and assumed the PSF as the Gaussian function, and denote the four-dimensional parameter of B_k by θ_k, which includes the one-dimensional rotation angle and the two dimensional translation, and the one-dimensional radius of the PSF.

The posterior of $\{\mathbf{x}_t\}_{t=1}^T$ is obtained as a multivariate Gaussian distribution again by introducing a Gaussian prior $p(\{\mathbf{x}_t\}_{t=1}^T)$:

$$p(\{\mathbf{x}_t\}_{t=1}^T) = \mathcal{N}(\mathbf{x}|\mathbf{0}, R \otimes I_{N_H}). \tag{3}$$

The mean of posterior μ, which is also the mode, is derived by

$$\mu = \left[(R\mathbf{a}_1) \otimes B_1^T \ \cdots \ (R\mathbf{a}_K) \otimes B_K^T\right] S^{-1}\mathbf{y}. \tag{4}$$

with

$$\begin{aligned} S = &\begin{bmatrix} (\mathbf{a}_1^T R\mathbf{a}_1)(B_1 B_1^T) & \cdots & (\mathbf{a}_1^T R\mathbf{a}_N)(B_1 B_N^T) \\ \vdots & & \vdots \\ (\mathbf{a}_N^T R\mathbf{a}_1)(B_N B_1^T) & \cdots & (\mathbf{a}_N^T R\mathbf{a}_N)(B_N B_N^T) \end{bmatrix} \\ &+ \beta I_{KN_L}. \end{aligned} \tag{5}$$

Though *mu* is the reconstructed hyperspectral image, The model parameters $\{\theta_k\}_{k=1}^K$ have to be determined before calculating Eq. (4). $\{\theta_k\}_{k=1}^K$ is determined by maximizing the log-marginalized likelihood $h(\{\theta_k\}_{k=1}^T)$:

$$\begin{aligned} &h(\{\theta_k\}_{k=1}^T) \\ &= \ln \int p(\{\mathbf{y}_k\}_{k=1}^K|\{\mathbf{x}_t\}_{t=1}^T) p(\{\mathbf{x}_t\}_{t=1}^T) d\mathbf{x}_1 \cdots d\mathbf{x}_T \\ &= -\frac{1}{2}\ln\det(2\pi S) - \frac{1}{2}\mathbf{y}^T S^{-1}\mathbf{y}. \end{aligned} \tag{6}$$

3 EXPERIMENTAL EVALUATION

A multispectral scanner was assembled with a monochromatic camera, LED lights, and six band-pass filters. The transmittance of the used filters had peaks at 420 nm, 450 nm, 500 nm, 530 nm, 550 nm and 600 nm with full width half maximum around 55 nm. The imaging subject was a Japanese painting which includes fine drawings and balanced colors shown in Figure 1. The size of the painting was 220 mm by 275 mm. The accuracy of the proposed method was evaluated in two areas illustrated in Figure 1 as well as in the whole area.

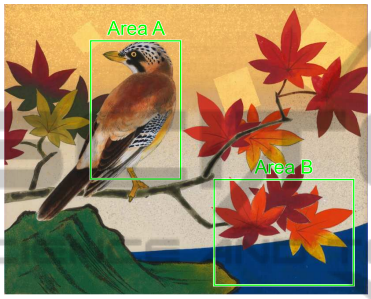

Figure 1: A Japanese painting used as a test object.

Seven sets of multispectral images were acquired with varying spatial resolutions: 200 to 500 DPI (dots per inch) at intervals of 50 DPI. Each band image in a multispectral image involved sub-pixel translation due to mechanical property of the scanner. The proposed Bayesian image reconstruction was applied to these seven multispectral images respectively and spectral reflectance from 400 nm to 700 nm was recovered. The rate of superresolution was set so as to recover a 600-DPI image of spectral reflectance from each multispectral image, namely set to 3, 2.4, 2, 1.71, 1.5, 1.33 and 1.2 for the acquired multispectral images with 200, 250, 300, 350, 400, 450 and 500 DPI respectively. The radius of PSF was set to 0.5 pixel at the acquired images, and the noise variance β was set to 1×10^{-6} where the brightness of band images was standardized up to 1.

For quantitative evaluation of the accuracy of recovered spectral reflectance, a 600-DPI multispectral image was acquired using the same scanner and object. Each band image was captured multiple times and carefully selected so that the acquired multispectral image included no position shifts, and spectral reflectance was then recovered by Wiener estimation. In this study this reflectance data was the reference to compare with spectral reflectance recovered by the proposed method. The root mean squared error (RMSE) of spectral reflectance and the average color difference were calculated for each recovered data.

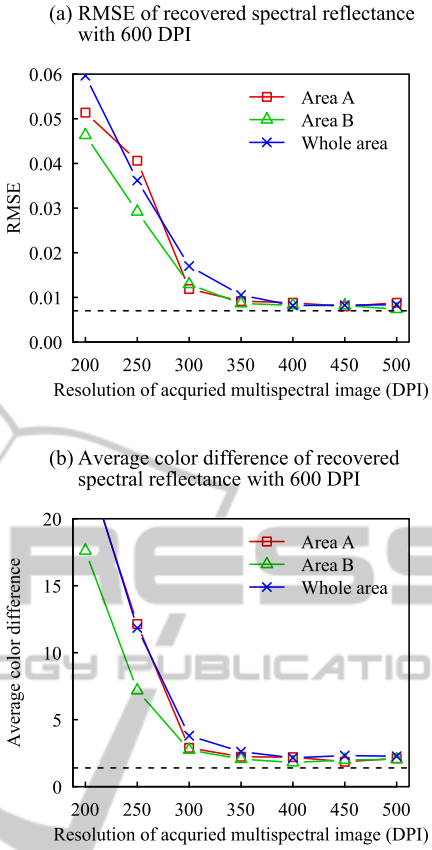

Figure 2: The errors of spectral reflectance of recovered 600-DPI images by the proposed method. Dashed lines illustrate the errors when spectral reflectance was recovered from multispectral image with 600 DPI and no misregistrations. Area A and B are depicted in Figure 1.

Figure 2 showed the result. Note that in the calculation of RMSE reflectance was represented as a fraction (not percentage), and the squared error was divided by the number the wavelength sampling points as well as by the number of color samples before taking the square root. In Figure 2, the background RMSE or the average color difference were added because they include some errors involving spectral reflectance recovery. These background errors were estimated by acquiring a multispectral image of an IT8 color chart where spectral reflectance of its 288 color patches was known. Figure 3 depicts color images reproduced from recovered spectral reflectance of the painting. Figure 2 indicated that there is a trade-off between accuracy and efficiency but both the RMSE and the average color difference were quite small when spectral reflectance was recovered with 600 DPI from multispectral images acquired with higher than or equal to 350 DPI. It means the rate of superresolution can be set to 1.71. Area A includes many fine lines and high-spatial-frequency components, but

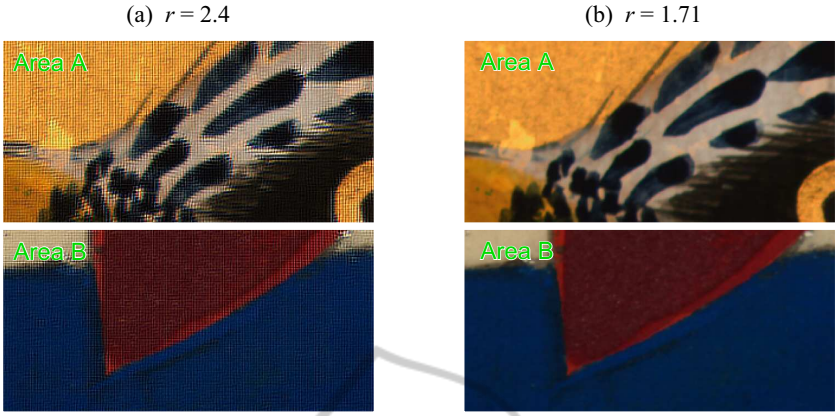

Figure 3: Color images reproduced from the recovered spectral reflectance. 600-DPI images were recovered from (a) 250-DPI images and (b) 350-DPI images, namely at the rate of superresolution $r = 1.71, 2.4$ respectively.

Area B includes few drawings. It had been expected that the errors would become much higher in Area A, but there was not a big difference between the results of these two areas. Figure 3 shows close-up color images reproduced from recovered 600-DPI images of spectral reflectance. There appears no false colors along edge lines. This means that registration of each band images was performed with high accuracy. In Figure 3 (a) the rate of superresolution r was set to 2.4, and there appeared grain-like noise. This could be because the number of sampling points in acquired image was not enough to recovery image with a certain high resolution and some pixels failed to be recovered. In Figure 3 (b) r was set to 1.71 and images were recovered successfully.

4 CONCLUSIONS

We tested experimentally the performance of Bayesian image reconstruction combined with spatial-superresolution and spectral reflectance recovery. Multispectral images of a Japanese painting was acquired with various spatial resolutions (less than or equal to 600 DPI) by using a typical 6-band multispectral scanner, then 600-DPI images and its spectral reflectance were recovered from each multispectral image. The experimental results showed that the spatial resolution could be increased by around 1.7 times and misregistrations between captured band images were completely removed. This indicated that the acquisition time of multispectral image can be reduced almost by one third (the negative 2nd power of the spatial resolution) and in addition the angle of view can be extended by around 1.7 times at the same time.

REFERENCES

DiCarlo, J. M. and Wandell, B. a. (2003). Spectral estimation theory: beyond linear but before Bayesian. *Journal of the Optical Society of America. A, Optics, image science, and vision*, 20(7):1261–1270.

Fukuda, H., Uchiyama, T., Haneishi, H., Yamaguchi, M., and Ohyama, N. (2005). Development of a 16-band multispectral image archiving system. *Proceedings of SPIE*, 5667:136–145.

Murayama, Y. and Ide-Ektessabi, A. (2012). Application of bayesian image superresolution to spectral reflectance estimation. *Optical Engineering*, 51(11):111713.

Pelagotti, A. and Mastio, A. D. (2008). Multispectral imaging of paintings. *IEEE Signal Processing Magazine*, 25(4):27–36.

Shimano, N., Terai, K., and Hironaga, M. (2007). Recovery of spectral reflectances of objects being imaged by multispectral cameras. *Journal of the Optical Society of America. A, Optics, image science, and vision*, 24(10):3211–3219.

Toque, J. A., Sakatoku, Y., and Ide-Ektessabi, A. (2009). Pigment identification by analytical imaging using multispectral images. *Image Processing ICIP 2009 16th IEEE International Conference*, pages 2861–2864.

Yamaguchi, M., Teraji, T., Ohsawa, K., Uchiyama, T., and Motomura, H. (2002). Color image reproduction based on multispectral and multiprimary imaging: experimental evaluation. *Proceedings of SPIE*, 4663:15–26.